Molecular Physics
Vol. 00, No. 00, Month 200x, 1–20

RESEARCH ARTICLE

The structure of strongly dipolar hard sphere fluids with extended dipoles by Monte Carlo simulations

Mónika Valiskó[†,*], Tibor Varga[†], András Baczoni[†], and Dezső Boda[†]

[†]*Department of Physical Chemistry, University of Pannonia, H-8201 Veszprém, PO Box 158, Hungary*

(*Received 00 Month 200x; final version received 00 Month 200x*)

We have investigated the structural change of dipolar hard sphere fluid while we change the dipole from an idealized point dipole (pDHS fluid) to a physically more realistic extended dipole (eDHS fluid) by increasing the distance d of the two point charges $\pm q$ while keeping the dipole moment $\mu = qd$ fixed. We discuss our results on the basis of the first- and second-rank orientational order parameters, angular distribution functions, chain-length distributions, and snapshots. At a low density, we have found chain formation with longer chains as the distance d is increased. At a high density, we have found phase transition from an orientationally ordered ferroelectric nematic phase (at low d) into an isotropic liquid containing chains (at large d).

1. Introduction

Strong dipolar interactions play an important role in technologically interesting physical systems such as ferrofluids [1], electrorheological liquids [2], or magnetic holes [3]. In the presence of external magnetic or electric field these systems tend to form strongly ordered stuctures. Some of them have an orientationally ordered structure even in the absence of an external field. This makes them important candidates in the creation of "intelligent" materials. While ferromagnetic fluids are well known, the ferroelectric phase, where the electrostatic forces alone produce an orientationally ordered nematic liquid, has not been found experimentally (although the theoretical possibility has been raised [4–6]).

Simulation and theoretical studies of polar fluids started with simple, general models of these molecules. More detailed models are needed to accurately describe a specific fluid, while reduced models are used with a few parameters to study general properties of polar fluids. The simplest models are those where a point dipole (pD) is placed in the center of a spherical core modelled by the hard sphere (HS), soft sphere (SS), or Lennard-Jones (LJ) potentials. We will refer to these systems as the pDHS, pDSS, and pDLJ systems, respectively. The latter system is commonly known as the Stockmayer fluid.

In this paper, our main goal is to study the effect of deviations from the idealized pD description of the charge distribution of the molecule. One way to do this is to add higher order terms to the multipole expansion. The other way, that we follow in this paper, is to model the actual three-dimensional charge distribution of the molecule. We take the first step and model the polar molecule by two partial charges $\pm q$ in a distance d from each other. This is called a real, physical, or

*Corresponding author. Email: valisko@almos.vein.hu

ISSN: 0040-5167 print/ISSN 1754-2278 online

DOI: 10.1080/0040516YYxxxxxxxx
http://www.informaworld.com

extended dipole in the literature. We follow Ballenegger and Hansen [7] and use the term "extended dipole" (eD). Thus, we will denote such an eD placed in the center of a HS, SS, or LJ core potential as eDHS, eDSS, or eDLJ fluid, respectively. Ballenegger and Hansen [7] studied the eDLJ and eDSS fluids, while we consider the eDHS system in this work (for the definition of the HS, pDHS, and eDHS potentials, see the next section).

Both simulation and theoretical [8, 9] methods prove that high density pDHS and pDSS fluids undergo a phase transition when the temperature is decreased. In the early 1990s, computer simulations of Wei and Patey [10–12] for the pDSS fluid and Weis and Levesque [13–15] for the pDHS fluid revealed the following phenomena. (1) At low densities, strongly dipolar spheres tend to form chains, where the dipoles are in head-to-tail position [13, 15]. (2) At high density, the dipoles form an orientationally ordered ferroelectric nematic phase in the absence of a depolarizing field (with the conducting boundary condition) [10, 11, 13, 14]. (3) When such a depolarizing field is present (sample surrounded by vacuum), oppositely polarized domains appear in the simulation cell [11, 14]. (4) Increasing the density, the system undergoes a ferroelectric liquid to ferroelectric solid phase transition [11, 14]. (5) In some cases, a columnar phase was found [11] where the chains form a spatial order perpendicular to them. Later, columnar order and transition temperatures were established with more careful simulation techniques using cluster moves and histogram reweighting [16, 17].

Furthermore, in contrast to theoretical predictions, simulations showed that there is no vapour-liquid equilibrium (VLE) in the pDHS and pDSS systems. At low temperatures, where one would expect VLE, ordered structures appear in the system. Leeuwen and Smit [18] showed for the pDLJ fluid that a minimum amount of attractive dispersion interaction is necessary to have VLE. This phenomenon was also found in the dipolar Yukawa fluid [19, 20].

In this work, we study the effect of making the dipole in the molecule more and more extended by increasing d and decreasing q while keeping the dipole moment $\mu = qd$ constant. Ballenegger and Hansen [7] studied the structural and dielectric properties of a high density eDLJ and eDSS systems this way. They used a smaller dipole moment than that which we use in this study, so they started from an isotropic liquid and found a transition into a hexagonal columnar phase above $d = 0.6$. We start from a ferroelectric liquid at small d, so our study supplements that of Ballenegger and Hansen.

More realistic models to represent the molecule's charge distribution have been considered in several studies [21–26]. The polarizability of the molecules was considered by several authors [27–29]. Orientationally ordered phases were found in the pDLJ fluid with and without molecular polarizability [30, 31], in a system with parallel point dipoles immersed in hard spheres [32], and in a rigid polyatomic model system with extended dipoles [33].

Here we study changes in the structure of the eDHS fluid as we increase the distance between the charges of the extended dipole while keeping the dipole moment fixed. We show that these structural changes are (1) the appearance of chains at a low density and (2) the disappearance of the ferroelectric phase at a high density. The changes in the structure were characterized by order parameters, chain-length distributions, various projections of the pair correlation function, and snapshots.

2. Model and Method

2.1. *Model*

The intermolecular potential of the eDHS fluid depends on the mutual positions $\mathbf{r}_{ij} = \mathbf{r}_i - \mathbf{r}_j$ and orientations Ω_i and Ω_j of the molecules: $u_{\mathrm{eDHS}}(ij) = u_{\mathrm{eDHS}}(\mathbf{r}_{ij}, \Omega_i, \Omega_j)$. It is a sum of two terms

$$u_{\mathrm{eDHS}}(ij) = u_{\mathrm{eD}}(ij) + u_{\mathrm{HS}}(r_{ij}) \tag{1}$$

where

$$u_{\mathrm{eD}}(ij) = q^2 \left[\frac{1}{|\mathbf{r}_i + d_2\mathbf{n}_i - (\mathbf{r}_j + d_2\mathbf{n}_j)|} - \frac{1}{|\mathbf{r}_i - d_2\mathbf{n}_i - (\mathbf{r}_j + d_2\mathbf{n}_j)|} - \frac{1}{|\mathbf{r}_i + d_2\mathbf{n}_i - (\mathbf{r}_j - d_2\mathbf{n}_j)|} + \frac{1}{|\mathbf{r}_i - d_2\mathbf{n}_i - (\mathbf{r}_j - d_2\mathbf{n}_j)|} \right], \tag{2}$$

is the interaction of the two extended dipoles (eD) in Gaussian units and

$$u_{HS}(r_{ij}) = \begin{cases} \infty \text{ for } & r_{ij} < \sigma \\ 0 \text{ for } & r_{ij} \geq \sigma, \end{cases} \tag{3}$$

is the hard sphere (HS) potential. The dipole moment of molecule i is modeled by partial charges of opposite signs $\pm q$ that are separated by a distance d inside the hard sphere of diameter σ, as shown in Fig. 1. In these equations, $r_{ij} = |\mathbf{r}_{ij}|$ is the distance of the centers of the spheres, $\mathbf{n}_i$ is the unit vector in the direction of the dipole moment of molecule i (characterizing orientation Ω_i), and $d_2 = d/2$. This equation does not contain the intramolecular interaction between the partial charges inside a single molecule. The charges are placed symmetrically by a distance d_2 from the center of the hard sphere. The dipole moment of such a molecule is [34]

$$\boldsymbol{\mu}_i = qd\mathbf{n}_i = \mu\mathbf{n}_i. \tag{4}$$

In our calculations, we simultaneously change q and d keeping the dipole moment $\mu = qd$ fixed. Thus, u_{eD} can be written as a product of μ^2 and a geometrical term depending on the mutual position and orientation of the molecules.

This term also carries the information about how far is the dipole from the idealized point dipole. When d is small, the limit of the u_{eD} potential is the point dipole-dipole (pD) potential :

$$u_{\mathrm{eD}} \to u_{\mathrm{pD}} \quad \text{if} \quad d \to 0 \quad \text{with} \quad \mu = \text{const.}, \tag{5}$$

where

$$u_{\mathrm{pD}}(ij) = -\mu^2 \frac{D(ij)}{r_{ij}^3}. \tag{6}$$

The following functions were introduced:

$$D(ij) = \frac{3(\mathbf{n}_i \cdot \mathbf{r}_{ij})(\mathbf{n}_j \cdot \mathbf{r}_{ij})}{r_{ij}^2} - \Delta(ij) \tag{7}$$

and

$$\Delta(ij) = \mathbf{n}_i \cdot \mathbf{n}_j. \tag{8}$$

These functions are rotational invariants; $\Delta(ij)$ is the scalar product of the unit vectors of two dipoles and $D(ij)$ is the angle dependent part of the pD potential.

2.2. *Pair distribution functions*

These functions appear in the series expansion of the pair correlation function of axially symmetric molecules:

$$g(ij) = \sum_{nml} h^{mnl}(r_{ij})\, \Phi^{mnl}(ij). \tag{9}$$

This expansion separates distance and angular dependence in such a way that the projections $h^{mnl}(r_{ij})$ depend only on the distance of particles and the projections $\Phi^{mnl}(ij)$ are rotational invariants.

The projection $h^{000}(r_{ij})$ is the usual radial distribution function:

$$h^{000}(r_{ij}) = \int g(ij) d\Omega_i d\Omega_j \,, \quad \text{with} \quad \Phi^{000} = 1. \tag{10}$$

In a fluid phase, $h^{000}(r_{ij}) \to 1$ when $r_{ij} \to \infty$ both in isotropic and nematic phases.

Other projections, also called angular correlation functions, carry information about the orientational behaviour of the fluid. The value of the $h^{112}(r_{ij})$ function is high if the interaction energy between two dipoles separated by a distance r_{ij} from each other is deep:

$$h^{112}(r_{ij}) = \frac{3}{2} \int D(ij) g(ij) d\Omega_i d\Omega_j \,, \quad \text{with} \quad \Phi^{112}(ij) = D(ij) \tag{11}$$

The value of the $h^{110}(r_{ij})$ function is high if the dipole moments of particles separated by a distance r_{ij} from each other tend to point in the same direction:

$$h^{110}(r_{ij}) = 3 \int \Delta(ij) g(ij) d\Omega_i d\Omega_j \,, \quad \text{with} \quad \Phi^{110}(ij) = \Delta(ij). \tag{12}$$

The value of the $h^{220}(r_{ij})$ function is high if the dipole moments of the particles separated by a distance r_{ij} from each other tend to be parallel (not necessarily pointing in the same direction):

$$h^{220}(r_{ij}) = \frac{5}{2} \int (3\Delta^2(ij) - 1) g(ij) d\Omega_i d\Omega_j \,, \quad \text{with} \quad \Phi^{220}(ij) = 3\Delta^2(ij) - 1. \tag{13}$$

If the system is isotropic, the latter three functions decay to 0 in the limit of $r_{ij} \to \infty$ indicating that there is no long range orientational order in the fluid.

2.3. *Order parameters*

In the nematic phase, on the contrary, the projections $h^{mn0}(r_{ij})$ obey the asymptotic behaviour:

$$\lim_{r\to\infty} h^{mn0}(r) = (2m+1)\left\langle P_m\right\rangle^2, \tag{14}$$

where $\langle P_m\rangle$ is the mth-rank order parameter and the brackets denote ensemble average. Particularly,

$$\lim_{r\to\infty} h^{110}(r) = 3\left\langle P_1\right\rangle^2 \tag{15}$$

and

$$\lim_{r\to\infty} h^{220}(r) = 5\left\langle P_2\right\rangle^2. \tag{16}$$

In the case of a long range orientational order, the functions $h^{110}(r)$ and $h^{220}(r)$ become constant at large separation. These constants are related to the first- and second-rank orientational order parameters that are computed in our simulations in an alternative way too. The second-rank order parameter $\langle P_2\rangle$ is the ensemble average of the largest eigenvalue of the instantaneous second-rank tensor

$$Q^{\alpha\beta} = \frac{1}{N}\sum_{i=1}^{N}\frac{1}{2}(3n_i^\alpha n_i^\beta - \delta^{\alpha\beta}), \tag{17}$$

where N is the number of particles in the simulation cell, n_i^α is the α-component of the unit vector $\mathbf{n}_i$, and $\delta^{\alpha\beta}$ is the Kronecker-delta. The corresponding eigenvector is the instantaneous director $\mathbf{P}$. The first-rank order parameter $\langle P_1\rangle$ (the normalized polarization) is the ensemble average of

$$P_1 = \frac{1}{N}\left|\sum_{i=1}^{N}\mathbf{n}_i\cdot\mathbf{P}\right|. \tag{18}$$

2.4. *Chain formation*

Strong dipoles tend two arrange in their minimum energy head-to-tail position, thus forming chains. We applied an energy criterion to define chains. Two dipoles are defined to be in the same chain if their interaction energy is lower than a prescribed value. In this study, we used the value $0.7\,u_{\mathrm{head-to-tail}}$, where

$$u_{\mathrm{head-to-tail}}(d) = -\frac{q^2}{1-d} - \frac{q^2}{1+d} + 2\frac{q^2}{1} = -2\frac{\mu^2}{1-d^2}, \tag{19}$$

is the lowest possible interaction energy of two dipoles: when they are in contact ($r_{ij}=1$) and in head-to-tail position ($\mathbf{n}_i = \mathbf{n}_j = \mathbf{r}_{ij}/r_{ij}$).

Thus, we can calculate the number of chains n_s having length s. The average chain length for a configuration is given by

$$l = \frac{\sum_s s n_s}{\sum_s n_s}. \tag{20}$$

The simulations produce ensemble averages for the average chain length $\langle l \rangle$ and the distribution of chain length $\langle n_s \rangle$ as a function of s.

2.5. *Monte Carlo simulations*

Canonical MC simulations were performed in cubic simulation cells of constant volume V at constant temperature T and at a fixed number of particles N. We used the standard Metropolis algorithm [35–37] with two kinds of MC moves. (1) A randomly-chosen particle was randomly displaced not too far from its original position. This kind of step is useful at high density, liquid-state systems. (2) Particle displacement in the whole simulation cell to a randomly-chosen position that is independent from the original position. We applied this step to equilibrate the low density system.

At low densities, after 30,000-50,000 MC cycles (an MC cycle involved N attempts to move a particle), the number of the successful displacements decreased considerably. When the chains are formed, the system is in a local energy minimum: it is practically frozen. Rarely accepted moves can make the sampling inefficient. To improve the sampling, we applied a double loop during the simulations. The internal cycle included an equilibration period and a production run. In the external cyle we repeated these relatively short runs starting from newly generated initial configurations. At the end we averaged the results of the production runs of the independent internal cycles.

In the case of the high density system, the initial configurations were generated in the following way: we started from a lattice, then we produced a disordered, isotropic, liquid-like state with a short simulation using a low dipole moment. Then, we increased the dipole moment to the high value used in the production run.

The long range corrections were treated with the reaction field (RF) method. In this method, the sample is considered to be surrounded by a dielectric continuum with a dielectric constant ϵ_{RF}. The charge induced on the boundary of the spherical sample and the surrounding dielectric exerts a force on the central dipole described by the potential of the reaction field

$$u_{\mathrm{RF}}(\Omega_1) = -\frac{2(\epsilon_{\mathrm{RF}}-1)}{2\epsilon_{\mathrm{RF}}+1}\frac{\boldsymbol{\mu}_1 \cdot \mathbf{M}}{R_{\mathrm{c}}^3}, \tag{21}$$

where $\boldsymbol{\mu}_1$ is the dipole moment of the central dipole, $\mathbf{M}$ is the total dipole moment of the sample, and R_{c} is the radius of the sample chosen to be the half width of the simulation cell.

The value of ϵ_{RF} strongly influences the behaviour of the system in the ferroelectric nematic phase. If ϵ_{RF} is high (or $\epsilon_{\mathrm{RF}} \to \infty$ in the case of the conducting or tin-foil boundary condition), $u_{\mathrm{RF}} = -2(\boldsymbol{\mu}_1 \cdot \mathbf{M})/R_{\mathrm{c}}^3$, which is a negative contribution if $\boldsymbol{\mu}_1$ is parallel to $\mathbf{M}$. It provides a strong polarizing field when the ferroelectric phase is formed, namely, the reaction field facilitates the formation of the orientationally ordered phase.

The value $\epsilon_{\mathrm{RF}} = 1$ (the sample is surrounded by vacuum), on the other hand, acts against the formation of long range order. (Note that in the case of Ewald summation a depolarization field appears in the case of $\epsilon_{RF} = 1$, which is absent for $\epsilon_{\mathrm{RF}} \to \infty$. In the reaction field method, a polarizing field appears for the latter case, absent in the former, with the same effect.) In this case, the system tends to form local structures while keeping the total polarization zero. Because the system has a large dielectric constant, using the tin-foil boundary condition is reasonable.

Therefore, we present our results for $\epsilon_{\rm RF} \to \infty$ in detail, while we briefly discuss our results for $\epsilon_{\rm RF} = 1$.

3. Results and Discussion

In this study, we use reduced quantities: the reduced density is $\rho^* = \rho\sigma^3$, where $\rho = N/V$, while the reduced dipole moment is $(\mu^*)^2 = \mu^2\sigma^3/kT$. Distances are given by choosing $\sigma = 1$ as the unit of distance so we define the following reduced quantities: $d^* = d/\sigma$ and $r^* = r/\sigma$. The state of the pDHS system can be fully defined by the values of ρ^* and $(\mu^*)^2$, while the additional parameter d^* (that characterizes the non-ideality of the dipole) is needed to fix the thermodynamic state of the eDHS system. The number of particles N or the volume V is also needed to fix the size of the system.

We studied a low density $\rho^* = 0.05$ and a high density $\rho^* = 0.8$ case, with dipole moments $(\mu^*)^2 = 3$ and $(\mu^*)^2 = 6$, respectively. Our goal was to study the effect of the non-ideality of the dipoles on the properties of the system by increasing d while keeping $\mu = qd$ constant.

3.1. *Low density*

At low density ($\rho^* = 0.05$), we started the process from a state where the pDHS system isotropic and no considerable chain formation is detected: $d^* = 0.001$ (which practically corresponds to the pDHS case) with dipole moment $(\mu^*)^2 = 3$. Then, we gradually increased the distance between the partial point charges of the eD to $d^* = 0.8$. The number of particles was 512 in these simulations. We applied the tin-foil boundary condition ($\epsilon_{RF} \to \infty$).

As the dipole was being made more and more non-ideal, longer chains appeared in the system. Figure 2a shows the distribution of the average chain length for various values of d^*. At small d^*, only associated dipole-pairs appeared (and a few triplets), while increasing d^* longer chains could be found. Based on these distributions, the average chain length was calculated using Eq. 20. The result is shown in Fig. 2b as a function of d^*. The average chain length increases with increasing d^*.

Chain-formation is also shown by the correlation functions $h^{000}(r)$, $h^{112}(r)$, and $h^{110}(r)$ (Fig. 3). High peaks appear at distances $r^* = 1$, 2, and 3 for larger d^*. The peaks indicate association of the particles at contact positions. The peaks in $h^{112}(r)$ indicate that particles with their associates have low energy mutual configurations at these positions. Furthermore, the peaks in the $h^{110}(r)$ functions indicate that the dipoles of the particle associates are parallel and point in the same direction. This is a clear footprint of chain formation. A visual representation of a randomly chosen configuration for $d^* = 0.8$ clearly shows the chains (Fig. 4).

The asymptotic behaviour of the correlation functions ($\lim_{r\to\infty} h^{000}(r) = 1$, $\lim_{r\to\infty} h^{112}(r) = 0$, and $\lim_{r\to\infty} h^{110}(r) = 0$) indicate that the system is still an isotropic fluid despite the chain formation. The system can be viewed as a mixture of chains of various lengths in a dynamical sense. The chains break up and reform, they exchange particles during the thermal motion, so the system cannot be considered as a mixture of polymers of fixed lengths in a static sense.

The above results for the low density system were expected. The interaction energy between two particles in head-to-tail position Eq. 19 becomes more attractive as d^* increases. In other words, additional attractive terms between dipole and higher-order moments (the next non-vanishing term is the octopole moment) appear as the charge distribution of the molecule becomes different from the pD.

4. High density

At a high density, on the contrary, we obtained surprising results. We expected that the enhanced attraction between extended dipoles in head-to-tail positions would make the formation of a ferroelectric nematic phase more probable. In this phase, chains would be formed, but they would be straight and parallel, thus producing a long range order in the liquid.

We chose the dipole moment $(\mu^*)^2 = 6$ at density $\rho^* = 0.8$ and increased d^* keeping $\mu = qd$ fixed as in the low density case. At this value of the dipole moment, the pDHS system formed a ferroelectric nematic phase using tin-foil boundary condition ($\epsilon_{\mathrm{RF}} \to \infty$). The boundary condition is important at high densities for the formation of long range orientational order. First, we present our results for $\epsilon_{\mathrm{RF}} \to \infty$, then we briefly discuss the case of $\epsilon_{\mathrm{RF}} = 1$. System size is also important at high densities. We will report our results using 620 particles, but we will also present an analyzis of system size dependence to show that system size effects did not influence our qualitative findings.

Figure 5 shows the order parameters as functions of d^*. The nonzero value of both $\langle P_1 \rangle$ and $\langle P_2 \rangle$ for small d^* indicates the formation of long range orientational order in the liquid. The order parameters increase with increasing d^* up to about $d^* = 0.4$ so the long range order becomes more stable. This is in agreement with the results of Hansen and Ballenegger [7] who reported a phase transition from an isotropic fluid phase to a ferroelectric columnar phase at the value $d^* \approx 0.64$ for the eDLJ fluid with a dipole moment smaller than that we used here.

Our dipole moment, nevertheless, is larger, so after a stabilization process of the long range orientational order, a sudden structural change occurs between $d^* = 0.4$ and 0.5. The order parameters drop to small values close to zero that implies that the long range orientational order vanishes for large d^* (the order parameters are finite due to the finite size of the simulation cell).

Thus, depending on the value of d^*, the system can be in two characteristically different phases. To understand the structure of the fluid in these phases, let us investigate the angular correlation functions. The radial distribution functions (not shown) behave as expected: they exhibit peaks at contact positions indicating strong association of particles and approach to 1 for $r \to \infty$ indicating that the system is a liquid.

Figure 6 shows results for the $h^{112}(r)$, $h^{110}(r)$, and $h^{220}(r)$ angular correlation functions for different values of d^*. For small values of d^*, these functions show a behaviour characteristic of a ferroelectric nematic phase as was found before for the pDHS fluid [14] and for the pDSS fluid [10, 11]. The $h^{110}(r)$ and $h^{220}(r)$ projections approach to their asymptotic values $3\langle P_1 \rangle^2$ and $5\langle P_2 \rangle^2$ as indicated by arrows in the figure. The ferroelectric nematic phase is illustrated in Fig. 7a, where a snapshot is shown for $d^* = 0.2$. The dipoles tend to point in the same direction; chains can be identified, but the system is otherwise a liquid without long range spatial order.

The curves for $d^* = 0.4$ are more structured with larger order parameters which raises the possibility of a columnar order. In this phase, there is a long range spatial structural order in the direction perpendicular to the chains/columns (the director). Therefore, the system is a liquid in parallel to the chains, while it is a crystal perpendicular to them. Such a phase has been reported before for dipolar fluids at low temperatures. Weis and Levesque [17] reported the appearance of a columnar phase for the pDHS fluid at $(\mu^*)^2 \geq 6.25$ for $\rho^* = 0.92$. They did not find the columnar phase in their earlier study [14] for $\rho^* = 0.84$ and $(\mu^*)^2 = 9$. Wei and Patey [11] reported a columnar phase for the pDSS fluid for $\rho^* = 0.7$ and

$(\mu^*)^2 = 9$. Ballenegger and Hansen [7] showed that a columnar ordering appears when the distance of the two point charges is above $d^* = 0.64$ in the eDLJ fluid for $\rho^* = 0.82$ and $(\mu^*)^2 = 2.88$. In our simulation for $d^* = 0.4$, investigation of snapshots did not reveal any columnar order. Decisive identification requires the calculation of the pair distribution functions parallel and perpendicular to the director, $h_{\parallel}(r)$ and $h_{\perp}(r)$. We did not compute these functions, so we do not pursue this question further in this study.

When d^* is increased further, $d^* \geq 0.5$, the nature of angular correlation functions changes dramatically. High peaks appear at positions $r^* = 1$, 2, and 3 indicating short-range correlation between the particles. The functions $h^{110}(r)$ and $h^{220}(r)$ approach 0 as $r \to \infty$ showing that the long range orientational order vanishes. These functions resemble those for low density (Fig. 3) where chains are formed. It implies that local structures with chain formation appear without any global orientation order. The absence of global order and the chains can be observed in Fig. 7b where a snapshot is shown for $d^* = 0.65$.

The energetic criterion for chain formation, which was mainly used in gas phase where the chains are distinct, can also be used in liquid phase [15] to show the distribution of chains of various lengths as d^* is varied. Figure 8 shows the chain length distribution for high density. The figure is quite similar to the low density case (Fig. 2b). Increasing d^*, longer chains appear in the system.

The structure of this liquid is also very similar to the low density counterpart: the fluid is like a mixture of polymers formed by the associating dipoles. The lengths and conformations of the chains vary during thermal motion, they are not "stable entities" [15].

Our qualitative conclusion (that a phase transition from a ferroelectric nematic to a chain-rich isotropic phase appears) does not depend on system size. Figure 9 shows results for the $h^{110}(r)$ function at different particle numbers for two values of d^*. Although some quantitative deviations can be seen, the qualitatively different behaviour of the function for $d = 0.2$ and 0.8 does not depend on N. Similar insensitivity to system size can be observed for the other projections too (data not shown).

When the sample is surrounded by vacuum, ($\epsilon_{\mathrm{RF}} = 1$), the polarizing reaction field is absent. As it was shown earlier [11, 14], the system tends to form locally oriented structures (domains) while maintaining a globally unpolarized state. In particular, simulations for the pDHS system at $\rho^* = 0.916$, $(\mu^*)^2 = 6.25$, and $N = 500$ produced two oppositely polarized domains [14]. We found a similar behaviour for the eDHS fluid for $d^* = 0.2$ using $N = 620$ particles. For this value of d^*, the $h^{110}(r)$ projection decays to zero for $r \to \infty$, while the $h^{220}(r)$ projection approaches a finite value. Interestingly, this behaviour vanishes when we increase system size. Even for $N = 864$ particles, we have not found the two oppositely polarized domains and both projections decay to zero. Our results imply that simulations for $\epsilon_{\mathrm{RF}} = 1$ are strongly dependent on system size.

For $d^* = 0.8$, we have found the same behaviour that we found in the case of the tin-foil boundary condition: formation of chains in local structures without any global order.

5. Conclusions

The physical reason of the phase transition at $d \approx 0.5$ is probably a result of the competition of three balancing forces: (1) the attraction between dipoles in head-to-tail positions, (2) the repulsion when they are in parallel positions, and (3) the

negative energy gained from the polarizing reaction field (for $\epsilon_{\rm RF} =\rightarrow \infty$) when the dipoles are aligned. When d is small, the repulsive contribution to free energy from the parallel dipoles is balanced by the third term. When d is increased, the second repulsive term increases but the third attractive term does not (the dipole moment does not change as d is increased because $\mu = qd$ is kept fixed). Thus, the second term cannot be balanced by the third term anymore. The other way to get rid of the parallel dipoles is to break up the aligned, parallel structure of the chains and to fold them up without a long range orientational order. The system becomes unpolarized; the third term vanishes, but the free energy is still minimized this way.

All these results imply that the molecules of strongly dipolar fluids – especially if we model them with partial charges located at certain sites – tend to associate into local structures like chains. They have a medium range pattern strongly dependent on boundary conditions and system size. Globally, they are not polarized in the absence of an external polarizing effect (the reaction field in our simulations provides this effect in some cases). This kind of association and locally ordered liquid structure are present in real liquids with large dipole moment. Chains were identified in liquid HF by Jedlovszky and Vallauri [38] using a more realistic model potential in molecular dynamics simulations. The most widely known example for strong local ordering in an otherwise isotropic liquid is water.

We conclude that modeling strongly polar fluids by extended dipoles reveales a behaviour not necessarily described by idealized point dipoles. Site-site potentials, used in force fields commonly applied in molecular dynamics simulations, or higher order terms in the multipole expansions might be necessary for more realistic description of the molecules' charge distribution. Furthermore, taking the polarizability of the molecules into account is probably needed to accurately describe the structural and dielectric properties of strongly polar fluids [28, 29].

Acknowledgment

This work was supported by the Hungarian National Research Fund (OTKA K68641) and the János Bolyai Research Fellowship. We are grateful to Douglas Henderson for his valuable comments.

References

[1] R. E. Rosensweig, Sci. Am. **247**, 124 (1982); *Ferrodynamics* (Cambridge University, New York, 1985).
[2] T. C. Halsey, Science **258**, 761 (1992); *Electrorheological Fluids*, edited by R. Tao (World Scientific, Singapore, 1992).
[3] A. T. Skjeltorp and G. Helgesen, Physica A **176**, 37 (1991).
[4] L. Lei, Mol. Cryst. Liq. Cryst. **146**, 41 (1987); L. M. Leung and L. Lei, ibid **146**, 71 (1987).
[5] P. P-Muhoray, M. A. Lee and R. G. Petshek, Phys. Rev. Lett. **60**, 2303 (1988).
[6] F. Biscarini, C. Zannoni and P. Pasini, Mol. Phys. **73**, 439 (1991).
[7] V. Ballenegger and J.-P. Hansen, Mol. Phys. **102**, 599 (2004).
[8] B. Groh and S. Dietrich, Phys. Rev. Lett. **72**, 2422 (1994).
[9] B. Groh and S. Dietrich, *Bulk and Surface Properties of Dipolar Fluids* in C. Caccamo *et al* (eds.) *New Approaches to Problems in Liquid State Theory*, 173-196. (Kluwer Academic Publishers, Amsterdam, 1999).
[10] D. Wei and G. N. Patey, Phys. Rev. Lett. **68**, 2043 (1992).
[11] D. Wei and G. N. Patey, Phys. Rev. A **46**, 7783 (1992).
[12] D. Wei and G. N. Patey, Phys. Rev. E **47**, 2954 (1993).
[13] J. J. Weis and D. Levesque, Phys. Rev. Lett. **71**, 2729 (1993).
[14] J. J. Weis and D. Levesque, Phys. Rev. E **48**, 3728 (1993).
[15] D. Levesque and J. J. Weis, Phys. Rev. E **49**, 5131 (1994).
[16] J. J. Weis and D. Levesque, J. Chem. Phys. **123**, 044503 (2005).
[17] J. J. Weis and D. Levesque, J. Chem. Phys. **125**, 034504 (2006).
[18] M. E. van Leeuwen and B. Smit, Phys. Rev. Lett. **71**, 3991 (1993).
[19] D. Henderson, D. Boda, I. Szalai, and Kwong-Yu Chan, J. Chem. Phys.**110**, 7348 (1999).

[20] I. Szalai, D. Henderson, D.Boda, and Kwong-Yu Chan, J. Chem. Phys.**111**, 337 (1999).
[21] A. Kachel, Z. Gburski, J. Mol. Struc. **480**, 349 (1999) and references therein.
[22] S. Calero, B. Garzo, and S. Lago, J. Chem. Phys. **118**, 11079 (2003).
[23] Yu. V. Kalyuzhnyi, G. Stell, M. L. Llanno-Restrepo, W. G. Chapman, and M. F. Holovko, J. Chem. Phys. **101**, 7939 (1994).
[24] S. C. McGrother, R. P. Sear, and G. Jackson, J. Chem. Phys. **106**, 7315 (1997).
[25] A. J. Perstin and M. Grunze, J. Chem. Phys. **106**, 7343 (1997).
[26] S. Lago, S. L-Vidal, B. Garzón, J. A. Mejs, J. A. Anta and S. Calero, Phys. Rev. E **68**, 021201-1 (2003). and references therein
[27] E. L. Pollock, B. J. Alder, and G. N. Patey, Physica A **108**, 14 (1981).
[28] M. Valiskó, D. Boda, J. Liszi and I. Szalai, Molec. Phys., **101**, 2309 (2003).
[29] M. Valiskó, D. Boda, J. Phys. Chem. B., **109**, 6355 (2005).
[30] J. Bartke, R. Hentschke, Mol. Phys., **104** 3057 (2006).
[31] J. Bartke, R. Hentschke, Phys. rev. E, **75** 061503 (2007).
[32] P. J. Camp, G. N. Patey, Phys. Rev. E. **60** (4): 4280 (1999).
[33] D. Q. Wei, Y. J. Wang, J. H. Hu, Z. Z. Gong, Y. X. Guo, Y. S. Zhu, Phys. Rev. E, **75**, 061702, (2007).
[34] J. D. Jackson, *Classical Electrodynamics* (3rd ed. Wiley, New York, 1999).
[35] N. Metropolis, A. W. Rosenbluth, M. N. Rosenbluth, A. H. Teller, E. Teller, J. Chem. Phys. **21**, 1087 (1953).
[36] M. P. Allen and D. J. Tildesley, *Computer simulation of liquids* (Oxford, New York, 1987).
[37] D. Frenkel and B. Smit, *Understanding molecular simulations* (Academic Press, San Diego, 1996).
[38] P. Jedlovszky and R. Vallauri, Mol. Phys. **93**, 15 (1998).

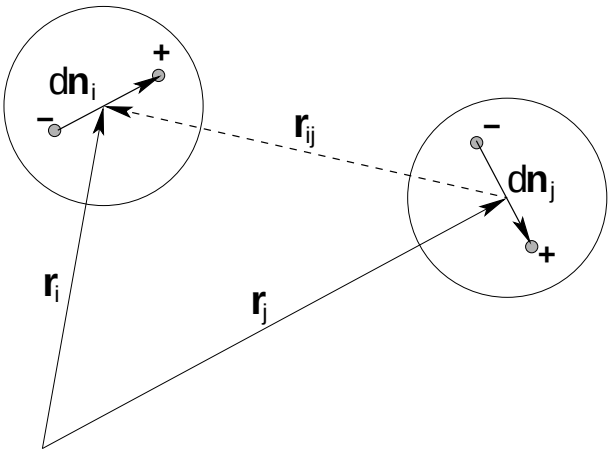

Figure 1. Illustration of the itermolecular potential. Partial charges of signs $\pm q$ are located centrally in a sphere of unit diamater in a distance of d from each other forming a dipole $\boldsymbol{\mu}_i = qd\mathbf{n}_i$, where $\mathbf{n}_i$ is the unit vector of the dipole.

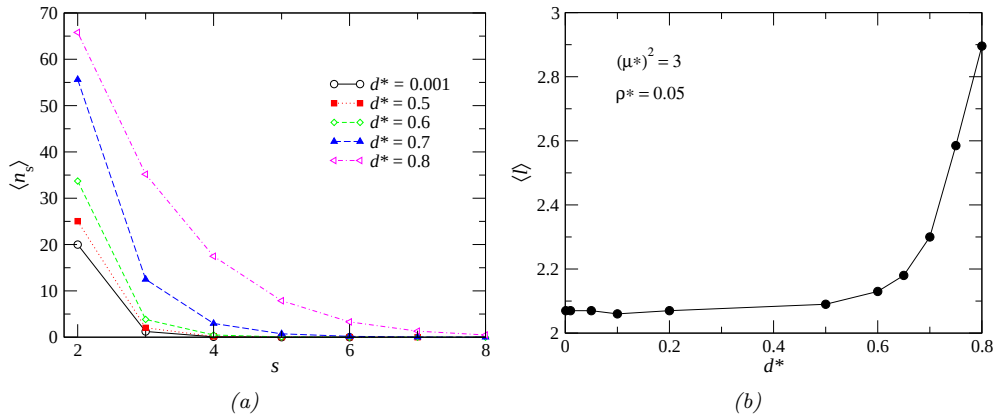

Figure 2. (a) Chain-length distributions at a low density ($\rho^* = 0.05$) for various values of d^*. (b) The average chain-length as a function of d^* computed from Eq. 20.

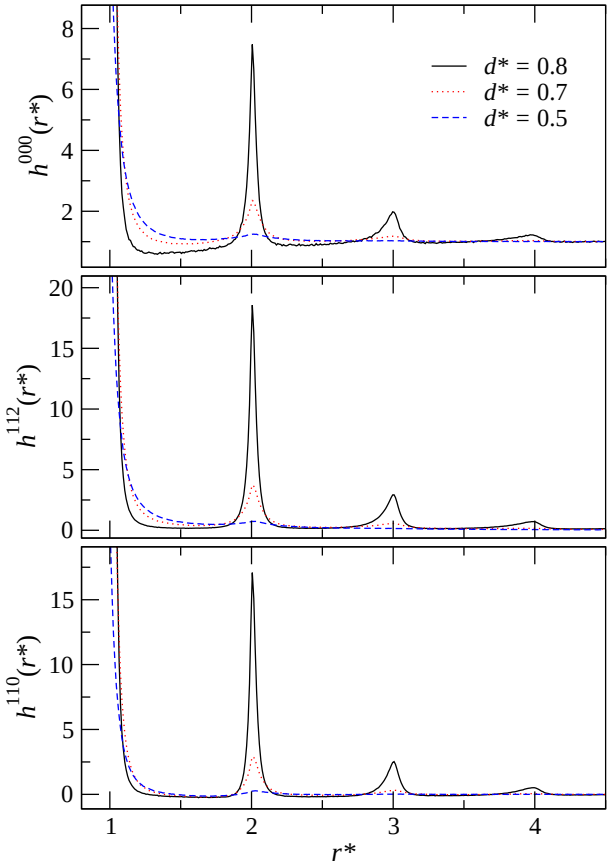

Figure 3. Projections $h^{000}(r)$, $h^{112}(r)$, and $h^{110}(r)$ of the pair-correlation function for low density ($\rho^* = 0.05$) for various values of d^*.

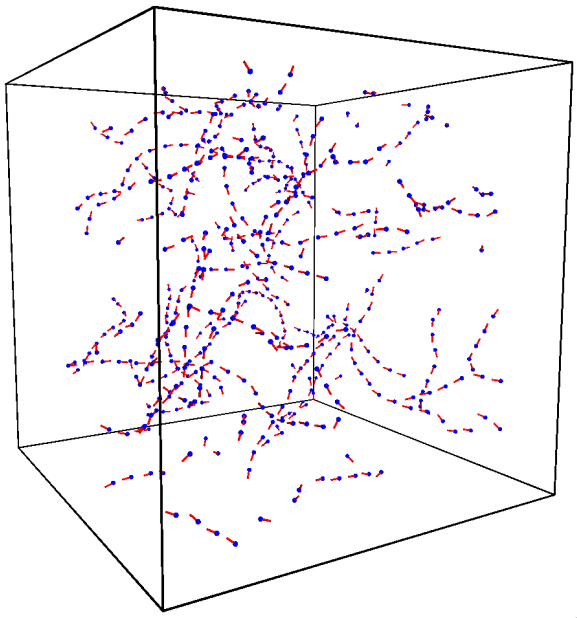

Figure 4. Snapshot of a randomly chosen configuration for $d^* = 0.8$ at a low density ($\rho^* = 0.05$). Blue dots represent the centers of the spheres, while the red rods show the orientations of the dipoles.

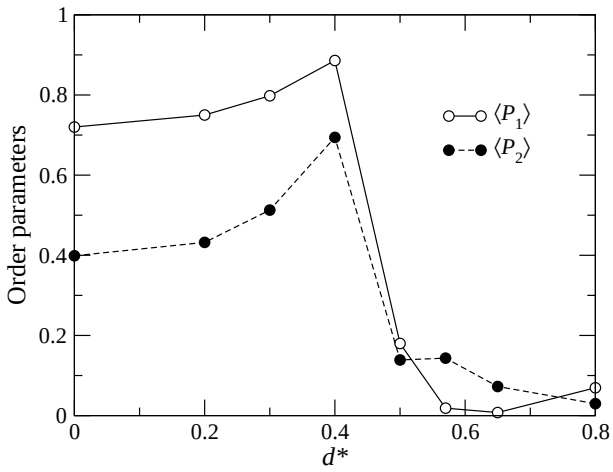

Figure 5. Order parameters as functions of d^* for a high density ($\rho^* = 0.8$).

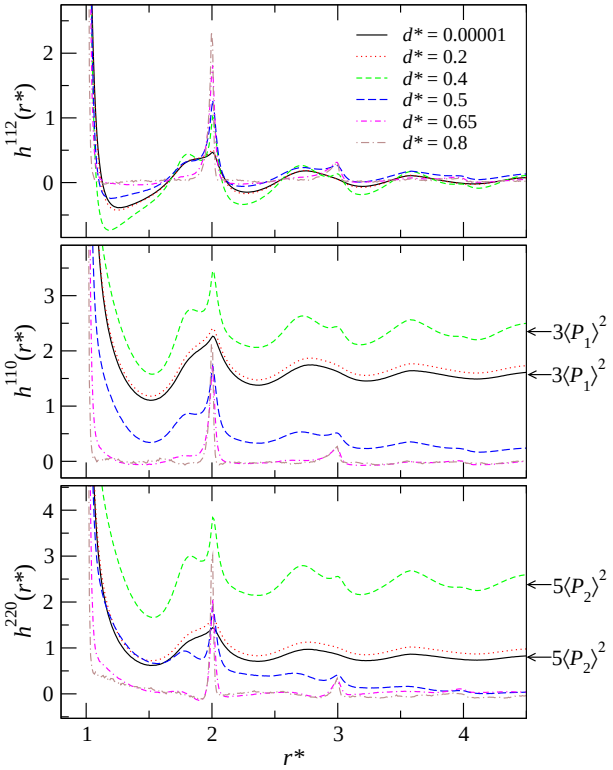

Figure 6. Projections $h^{112}(r^*)$, $h^{110}(r^*)$, and $h^{220}(r^*)$ of the pair-correlation function for a high density ($\rho^* = 0.8$) for various values of d^-.

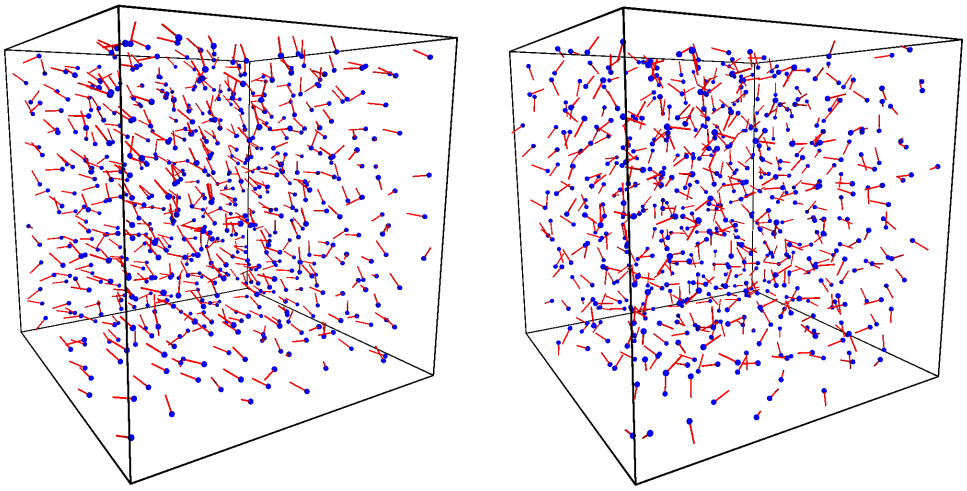

(a) *(b)*

Figure 7. Snapshot of randomly chosen configurations for (a) $d^* = 0.2$ and (b) $d^* = 0.8$ at a high density ($\rho^* = 0.8$). Blue dots represent the centers of the spheres, while the red rods show the orientations of the dipoles.

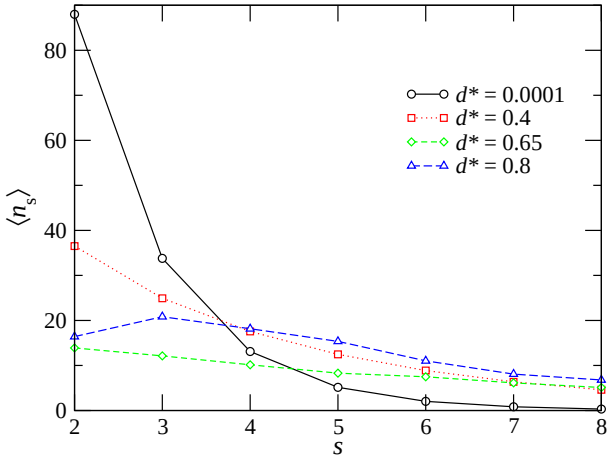

Figure 8. Chain-length distributions at a high density ($\rho^* = 0.8$) for various values of d^*.

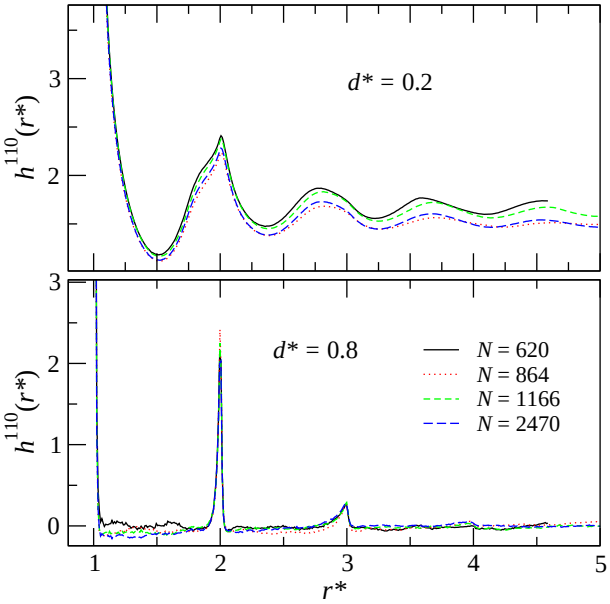

Figure 9. System size dependence of the projection $h^{110}(r^*)$ for various values of d^* at high a density ($\rho^* = 0.8$) using tin-foil boundary condition ($\epsilon_{\mathrm{RF}} \to \infty$). Various lines represent various numbers of particles as indicated in the figure.